JAERI-M
89-226

ELECTRON TEMPERATURE PROFILE MEASUREMENT USING THE FILTER ABSORPTION METHOD IN JT-60

January 1990

Keisuke NAGASHIMA, Takeo NISHITANI and Hiroshi TAKEUCHI

日本原子力研究所
Japan Atomic Energy Research Institute

JAERI-Mレポートは，日本原子力研究所が不定期に公刊している研究報告書です。
入手の問合わせは，日本原子力研究所技術情報部情報資料課（〒319-11茨城県那珂郡東海村）あて，お申しこしください。なお，このほかに財団法人原子力弘済会資料センター（〒319-11茨城県那珂郡東海村日本原子力研究所内）で複写による実費頒布をおこなっております。

JAERI-M reports are issued irregularly.
Inquiries about availability of the reports should be addressed to Information Division Department of Technical Information, Japan Atomic Energy Research Institute, Tokai-mura, Naka-gun, Ibaraki-ken 319-11, Japan.

編集兼発行　日本原子力研究所
印　　刷　㈱高野高速印刷

Electron Temperature Profile Measurement Using the Filter Absorption Method in JT-60

Keisuke NAGASHIMA, Takeo NISHITANI and Hiroshi TAKEUCHI

Department of Large Tokamak Research
Naka Fusion Research Establishment
Japan Atomic Energy Research Institute
Naka-machi, Naka-gun, Ibaraki-ken

(Received December 20, 1989)

The electron temperature profile was measured in JT-60 from the two arrays of 16 channel PIN photo-diodes arranged in parallel using the filter absorption method. From the error estimation of this method, especially for the impurity line radiation, the error was considered to be 10-20%. These values were confirmed by the comparison with the other measurements and this method was confirmed to be useful as the measurement of the electron temperature profile except for the very low density discharge below $\bar{n}_e=1.5\times10^{19}$ m^{-3}.

Keywords: JT-60, Soft X-ray, Electron Temperature, PIN Photo-diode, Filter Absorption Method, Line Radiation

ＪＴ－６０における吸収膜法による電子温度分布測定

日本原子力研究所那珂研究所臨界プラズマ研究部
永島　圭介・西谷　健夫・竹内　　浩

（１９８９年１２月２０日受理）

ＪＴ－６０において，２列１６チャンネルに配置したＰＩＮダイオード検出器を用いて，吸収膜法により電子温度分布を測定した。吸収膜法を用いた場合の誤差評価を，特に不純物の共鳴線について実施した結果，誤差は１０－２０％程度であることが分かった。この値は，本測定と他の測定法から得られた結果を比較することにより確認でき，線平均電子密度が $1.5 \times 10^{19}\ m^{-3}$ 以下の低電子密度領域を除いて，本測定法が十分利用できることが確認された。

那珂研究所：〒311－01 茨城県那珂郡那珂町大字向山801－1

Contents

目　　次

1. INTRODUCTION

As a diagnostic method for the high temperature plasma, the measurement of the soft x-ray intensity is very useful because it provides various informations about the plasma behaivors and has a high temporal and spatial resolutions and a simplicity of the equipment. So, in the many tokamaks this method has widely used to investigate the magnetohydrodynamic behaivors like sawtooth ocsillations[1] and disruptions[2].

The filter absorption method[3] is the very simple technique for the estimation of electron temperature. In this method the electron velocity is assumed to have a maxwellian distribution, so the electron temperature can be obtained easily from the intensity ratio through the different thickness filters. But the measured soft x-ray spectrum is distorted from the maxwellian spectrum due to the line radiations of impurities and the high energy tail generated from the non-maxwellian high energy electron like runaway electron. Moreover, the measured intensity is the chord integrated power, so the emissivity has to be calculated using the inversion technique.

Recently, this method applied to TFTR tokamak plasma successfully[4]. In JT-60, this method is more suitable because of its lower impurity levels with the diverted plasma. First, we refined the theoretical procedure to make clear the line radiation effect in Sec.2. The equipment is shown in Sec.3 and the error estimation of this method is discussed in Sec.4. In Sec.5 the experimental results are presented briefly and the conclusion is described in Sec.6.

2. THEORETICAL PROCEDURE

The soft x-ray emission from plasma consists of the continuum spectrum and the line radiations. Using the enhanement factor ζ which represents the multiplication for the pure hydrogen bremsstrahlung, the continuum energy spectrum is written[5,6] as,

$$\frac{dP_{con}(T_e,h_\nu)}{dh_\nu} = 3.0\times10^{-15}\zeta\, g_{ff,H} n_e^2 T_e^{-1/2} \exp(-h_\nu/T_e) \qquad (1)$$

[keV/keV cm^3 sec]

where n_e, T_e and h_ν are the electron density, the electron temperature and the photon energy, respectively. $g_{ff,H}$ represents the free-free gaunt factor of hydrogen averaged over a maxwellian distribution. The line radiation power of the i-transition of the impurity is

$$P_i = E_i\ (n_i/n_e)\ n_e^2\ \langle\sigma v\rangle_i \qquad [keV/cm^3\ sec] \qquad (2)$$

where n_i, E_i are the impurity density and the transition energy. $\langle\sigma v\rangle_i$ represents the total rate coefficient of the i-transition averaged over a maxwellian distribution. So the energy spectrum of the line radiation is given by

$$\frac{dP_i(T_e,h_\nu)}{dh_\nu} = E_i(n_i/n_e)\ n_e^2\ \langle\sigma v\rangle_i\ \delta(E_i-h_\nu) \qquad (3)$$

[keV/keV cm^3 sec]

where δ represents the delta function. Using the eqs.(1) and (3), the detected soft x-ray power is written as,

$$P_{det} = \int ds \int dh_\nu \varepsilon_f \varepsilon_d S_d \Delta\Omega/4\pi \left\{ \frac{dP_{con}}{dh_\nu} + \sum_i \frac{dP_i}{dh_\nu} \right\} \qquad (4)$$

[keV/sec]

where ε_f, ε_d, S_d and $\Delta\Omega/4\pi$ represent the filter transparency, the detector efficiency, the detector sensitive area and the solid angle, respectively. The second term in the bracket is the summation of the

dominant line radiations in the sensitive region of the detection efficiency. The first integral represents the viewing chord integral along the line of s. So, the detected line integral power is rewritten as,

$$P_{det} = S_d \Delta\Omega/4\pi \int ds \; g(r) \tag{5}$$

$$g(r)=3.0\times10^{-15} n_e(r)^2 \zeta(r) \; H(T_e,\eta_i) \qquad [keV/cm^3 \; sec] \tag{6}$$

where η_i is the relative impurity density defined by $\eta_i=(n_i/n_e)/\zeta$ and the function $H(T_e,\eta_i)$ is written as follows,

$$H(T_e,\eta_i) = T_e(r)^{-1/2} F(T_e) + \sum_i G(E_i)\eta_i \langle\sigma v\rangle_i'' \tag{7}$$

$$F(T_e) = \int dh_v \varepsilon_f(h_v)\varepsilon_d(h_v) \; \exp(-h_v/T_e) \; g_{ff,H}(T_e,h_v) \tag{8}$$

$$G(E_i) = \varepsilon_f(E_i) \; \varepsilon_d(E_i) \; E_i \tag{9}$$

where $\langle\sigma v\rangle_i''=\langle\sigma v\rangle_i/3.0E\text{-}15$. $H(T_e,\eta_i)$ is a function of the electron temperature, the absorbing filters and the relative impurity density η_i, so the intensity ratio of different thickness filters, $g_1(r)/g_2(r)$, is depending only on the electron temperature and η_i.

To obtain the solution of eqs.(6) to (9), the general least square method is used as follows,

$$S(x) \equiv \sum_{j=1}^{J} \left\{ y_j - \sum_{i=0}^{I} a_i f_{ji}(x) \right\}^2 \Rightarrow \min \tag{10}$$

where J is a number of the measured data and j represents the filter number. i=0 and i>0 correspond to the continuum and line radiations, and I is a number of the considering lines. The relation between eq.(10) and eqs.(6)-(9) is written in the appendix as $x=T_e$, $y_j=g_j$. So, the minimum value of S(x) can be found by changing the value of x.

3. EQUIPMENT

To measure a soft x-ray profile, 62 PIN photo-diodes are equiped on JT-60[7] as shown in Fig.1. The 62 detectors are divided into the three arrays. One views the under half of the plasma cross section by the 30 viewing chords. The another two arrays are arranged in parallel with each other and view the upper half of the same cross section by the 16 viewing chords. The spatial resolution is about 5 cm for the lower array and about 6 cm for the upper two arrays.

The PIN detector used in this system has the area of 10x10 mm^2, the depletion layer thickness of about 130 μm and the surface dead layer thickness of under 0.2 μm. The cut off energy corresponding to the surface dead layer is about under 0.4 keV.

In front of the detectors the remote controllable absorption filters are arranged and are able to select the appropriate x-ray energy range. The filter thickness and its cut off energy are shown in Table 1. The detection efficiency including the filter transparency is given by,

$$\varepsilon(h_\nu) = \varepsilon_f(h_\nu)\,\varepsilon_d(h_\nu)$$

$$= \exp(-\rho_f \mu_f t_f)\,\exp(-\rho_1 \mu_1 t_1)\,\{1-\exp(-\rho_2 \mu_2 t_2)\} \qquad (11)$$

where ρ, μ, t are the mass density, the mass absorption coefficient and the thickness, respectively. The subscripts of f, 1, 2 represent the filter, the detector surface dead layer and the effective sensitive layer (which is assumed to be equal to the depletion layer). And the calculated efficiency given by eq.(11) is shown in Fig.2.

The current generated by the absorbed x-ray energy in the PIN diode is amplified by the I/V convertor and digitized with the sampling frequency of 25 kHz. The detected soft x-ray power is given by,

$$P_{det} = \varepsilon\, V_{out}/G_{FB} \qquad [W] \qquad (12)$$

where ε is the averaged energy generating one electron-hole pair in eV unit. V_{out} and G_{FB} are the output voltage and the feedback gain of the I/V convertor.

4. ERROR ESTIMATION

For the estimation of electron temperature using the filter absorption method, the main origins of error are considered to be the impurity line radiation, the inversion of chord integrated data and the spectrum distortion from a maxwellian distribution. Moreover, the following points must be considered. The soft x-ray intensity ratio should be sensitive to electron temperature, so the difference between the filter cut off energies should be large. But the enough signal cannot be obtained with the filter of high cut off energy. To avoid the line radiations from light impurities like carbon and oxygen, the lower cut off energy must be over about 1 keV. To avoid the effect of the high energy tail (non-maxwellian effect), the adequate thin detector should be used.

In the following subsections, the above mentioned effects are considered respectively.

4.1 Line Radiation Effect

To make clear the effect of line radiation, the ratio of the soft x-ray intensity including the line radiation to the non-including (the ratio of the first and second term to the only first term in eq.(7)) are calulated in the case of titanium Kα-line. The dependence of the ratio in the case of $\eta_i=1.0\times10^{-5}$ on the beryllium filter thickness is shown in Fig.3. As increasing the filter thickness, the effect becomes remarkable and when the filter cut off energy is near the transition energy of titanium Kα-line, the ratio becomes maximum. Also, the electron temperature dependence of the ratio on the parameter of the beryllium filter thickness is shown in Fig.4. From these figures, this effect should be considered in the case of filter thickness over 200 μm for titanium Kα-line.

The several methods for avoiding the effect of line radiation are considered. One is the use of the unique filter which has the K-absorption edge on the line[4]. Secondly, this effect can be esitimated using the other diagnostic data like the pulse height analysis or the spectroscopic measurement of soft x-ray. Lastly, this effect can be

compensated using the multi-filter method where the adequate filter set is necessary to estimate the relative impurity densities.

In JT-60, the dominant metal impurities are titanium, chromium and nickel[6] and the value of η_i is about or smaller than 1.0×10^{-5} as can be seen in Fig.5 for the case of titanium, whuch is measured with the soft x-ray pulse height analysis. The error due to the line radiation is calculated using 25 μm and 250 μm beryllium filters. Figure 6 is the case of titanium and Figure 7 is the case of nickel. The effects of line radiations are different in the two cases due to the differece of the energy of Kα-lines. In the case of titanium, the error is maximum at about 1.3 keV and its value is about under 10% from Fig.5 except for the case of very low density discharges. The error due to nickel is several times lower than one due to titanium because nickel density is 2-5 times lower than titanium density in JT-60[6] and its effect is lower under about 5.0 keV.

4.2 Chord Integrated Effect

The detected intensity is the chord integrated value and it includes the effect of broadening of the viewing angle. Especially, for the peripheral channels the gradients of the soft x-ray emission become large, so its intensity ratio is considerably different from the case of the ideal chord integral. In order to include the effect of broadening of the viewing angle, the Wiener's back filter method[8] is applied as the inversion technique.

The detected chord integrated values are inverted to the emissivity on the magnatic surface geometry which is obtained by the magnetic fitting. So, we have to consider the geometrical error and the spatial asymmetry of the soft x-ray emission. The error from these effects was simulated using the test data for the several test cases and it was found to be about 10% in the central region and 10-20% in the peripheral region.

4.3 Non-maxwellian Effect

If the electron velocity distribution is not maxwellian and the high energy tail exists like in the case of lower hyblid current drive or runaway discharge, the two individual effects can be seen in the soft x-ray spectrum. One is the high energy tail over the energy range of several times larger than the thermal temperature and the other is the enhancement of the resonance line radiations of impurities. The latter is more dominant for the estimation of electron temperature.

5. EXPERIMENTAL RESULTS

In this section, it is shown the experimental results obtained in JT-60 using the filter absorption method. From the estimation described in the above section, we can find the filter pair of 25 μm and 250 μm as the optimum one in our system. So, this pair is used in the following results.

The time evolution of the measured electron temperature profile is shown in Fig.8. The discharge is 2.0 MA plasma current, 4.5 T toroidal field, and 18 MW neutral beam heating power. The line averaged electron density is about $7.5 \times 10^{19} m^{-3}$, and the effective safety factor q_{eff} is 3.24. In the central region the obvious sawtooth oscillation can be seen and its inversion radius is about 29 cm, which satisfies the approximate relation of $r_s/a_p = q_{eff}^{-1}$[9]. The radius of the outermost viewing channel is about 80 cm and so in the outer region of this radius the electron temperature cannot be estimated. The electron temperature profiles of one sawtooth evolution are shown in Fig.9.

The comparision of the measured electron temperature profile between the filter absorption method and the thomson scattering method can be seen in Fig.10. The shown error of the thomson scattering is statistical and the two are in good agreement with each other except for the region over r=80 cm. The comparision of the central electron temperature between the two methods is shown in Fig.11. The broken lines represent the 10% deviations and the almost points are within this range. The shown points are obtained in the various plasma conditions of 1.5-3.0 MA plasma current, 3.5-4.5 T toroidal field, $1.5\text{-}10.0 \times 10^{19} m^{-3}$ line averaged electron density, ohmic and neutral beam heated plasma. Also, the comparision of the peripheral electron temperature at r=64 cm is shown in Fig.12. In this case the several points are without the range of 10% deviations, and it is considered to be due to the effect of broadening of the viewing angle described as before.

The comparision of the central electron temperature between the filter absorption method and the soft x-ray pulse height analysis (PHA) is shown in Fig.13. The sampling time of PHA is 100msec, so

the maximum and minimum values of the filter absorption method in this time interval are shown, which correspond to the top and bottom values of the sawtooth oscillations. The statistical error for the estimation of electron temperature by PHA is in the range of 10 to 20%.

6. CONCLUSION

To measure the electron temperature profile using the filter absorption method, the two arrays of 16 channel PIN photo-diodes were equipped on JT-60. After refining the theoretical procedure, the error estimation was performed for the impurity line radiation and the chord integrated effect. From this estimation, the electron temperature profile could be measured in the error range of about 10-20%, except for the very low density discharge below $\overline{n_e}=1.5\times10^{19}$ m^{-3} and the non-maxwellian discharge where the effect of line radiation was remarkable. The measured electron temperature profile were well in good agreement with ones from the other measurements. This method have the merits of the high spatial and temporal resolutions, but it is necessary to assume a symmetry of the soft x-ray emission on the magnetic surface and a maxwellian distribution of electron velocity. These assumptions limits the application of the filter absorption method in the experimental conditions.

ACKNOWLEDGEMENTS

The authers would like to express their gratitude to the members of JT-60 team and Drs. M. Yoshikawa, M. Tanaka, S. Tamura and A. Funahashi for their continuous supports and fruitful suggestions.

6. CONCLUSION

To measure the electron temperature profile using the filter absorption method, the two arrays of 16 channel PIN photo-diodes were equipped on JT-60. After refining the theoretical procedure, the error estimation was performed for the impurity line radiation and the chord integrated effect. From this estimation, the electron temperature profile could be measured in the error range of about 10-20%, except for the very low density discharge below $\overline{n_e}=1.5\times10^{19}$ m^{-3} and the non-maxwellian discharge where the effect of line radiation was remarkable. The measured electron temperature profile were well in good agreement with ones from the other measurements. This method have the merits of the high spatial and temporal resolutions, but it is necessary to assume a symmetry of the soft x-ray emission on the magnetic surface and a maxwellian distribution of electron velocity. These assumptions limits the application of the filter absorption method in the experimental conditions.

ACKNOWLEDGEMENTS

The authers would like to express their gratitude to the members of JT-60 team and Drs. M. Yoshikawa, M. Tanaka, S. Tamura and A. Funahashi for their continuous supports and fruitful suggestions.

REFERENCE

[1] VON GOELER, S., STODIEK, W., SAUTHOFF, N.R., Phys. Rev. Lett. 33 (1974) 1201
[2] KADOMTSEV, B.B., Plasma Physics and Controlled Fusion 26 (1984) 217
[3] DONALDSON, T.P., Plasma Phys. 20 (1978) 1279
[4] KIRALY, J., BITTER, M., EFTHIMION, P., VON GOELER, S., GREK, B., HILL, K.W., JOHNSON, D., McGUIRE, K., SAUTHOFF, N., SESNIC, S., STAUFFER, F., TAIT, G., TAYLOR, G., Nucl. Fusion 27 (1987) 397
[5] SILVER, E.H., BITTER, M., BRAU, K., EAMES, D., GREENBERGER, A., HILL, K.W., MEADE, D.M., RONEY, W., SAUTHOFF, N.R., VON GOELER, S., Rev. Sci. Instrum. 53 (1982) 1198
[6] NISHITANI, T., NAGASHIMA, K., TAKEUCHI, H., JAERI-M 87-011
[7] NAGASHIMA, K., NISHITANI, T., TAKEUCHI, H., The Journal of the Japan Society of Plasma Science and Nuclear Fusion Research Vol.59 (1988) 215
[8] YAMASHITA, Y., JAERI-M 87-206
[9] SHIRAI, H., NAGASHIMA, K., NISHITANI, T. and JT-60 Team, JAERI-M 87-014

Table 1 Filter thickness and its cut off energy

	filter thickness	cutoff energy
upper (A)	Be $25.0^{+0.5}_{-1.5}$ μm	1.4 keV
	Be $250.0^{+10.0}_{+1.0}$ μm	2.9 keV
	Be $1000.0^{+56.0}_{+49.0}$ μm	4.5 keV
	Al $500.0^{+10.0}_{-10.0}$ μm	15.2 keV
upper (B)	Be $25.0^{+0.5}_{-1.5}$ μm	1.4 keV
	Be $500.0^{+49.0}_{+32.0}$ μm	3.6 keV
	Al $50.0^{+4.0}_{-0.0}$ μm	6.9 keV
	Al $150.0^{+10.0}_{-0.0}$ μm	10.1 keV
lower	Be $25.0^{+1.5}_{-1.5}$ μm	1.4 keV
	Be $250.0^{+10.0}_{+1.0}$ μm	2.9 keV
	Be $1000.0^{+25.0}_{-6.0}$ μm	4.5 keV
	Al $150.0^{+10.0}_{-0.0}$ μm	10.1 keV

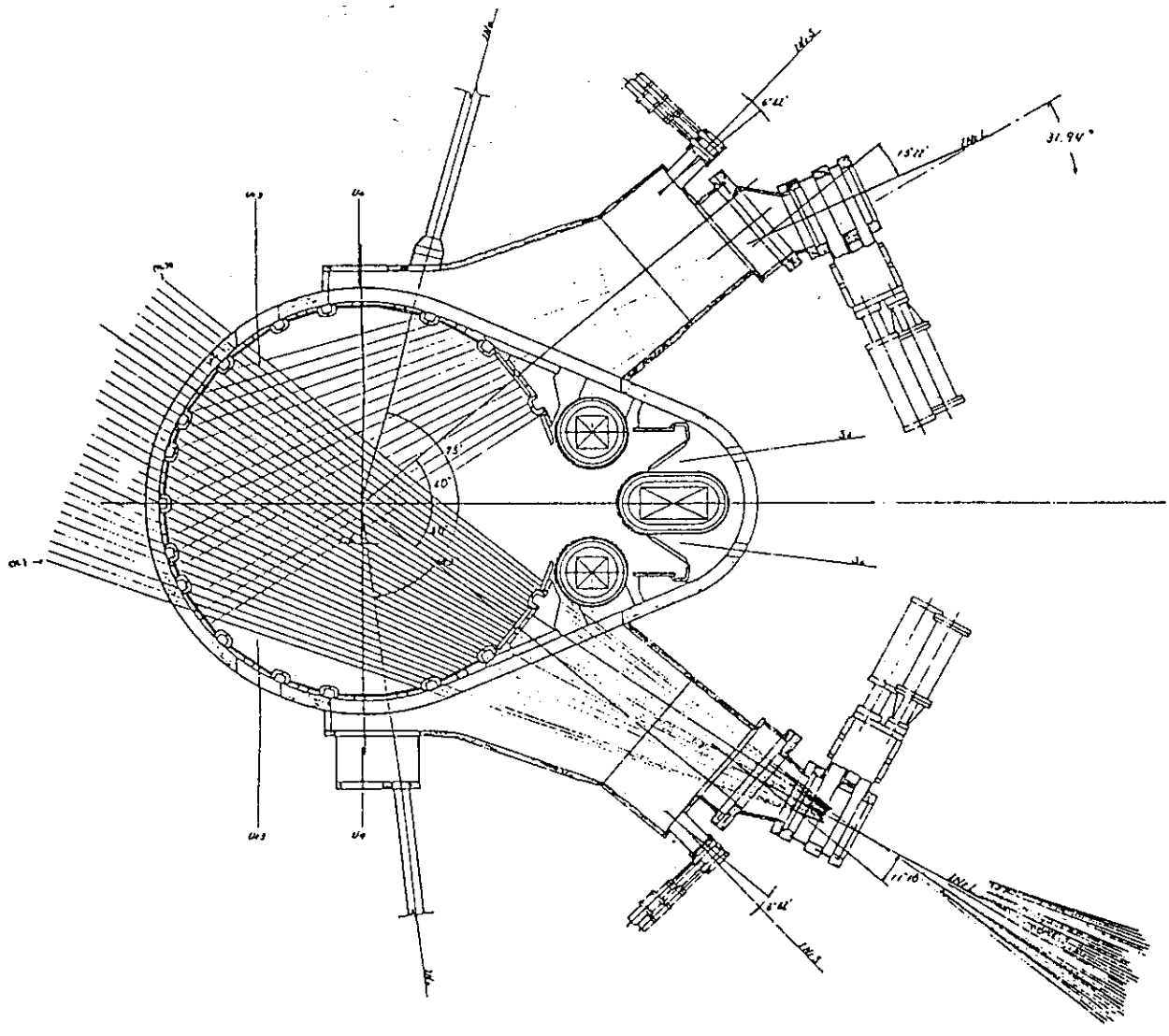

Fig.1 The poloidal cross section of JT-60 and the viewing chords of soft x-ray detectors.

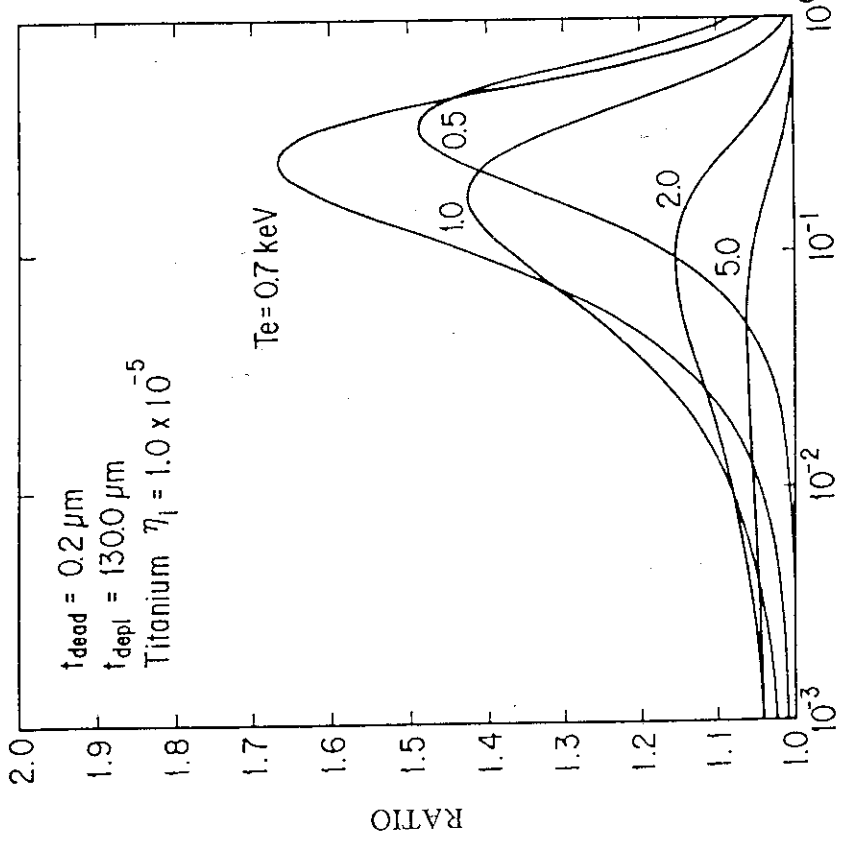

Fig.3 The dependence on the beryllium filter thickness of the ratio of the soft x-ray intensity including the line radiation to the non-including in the case of titanium Kα-line.

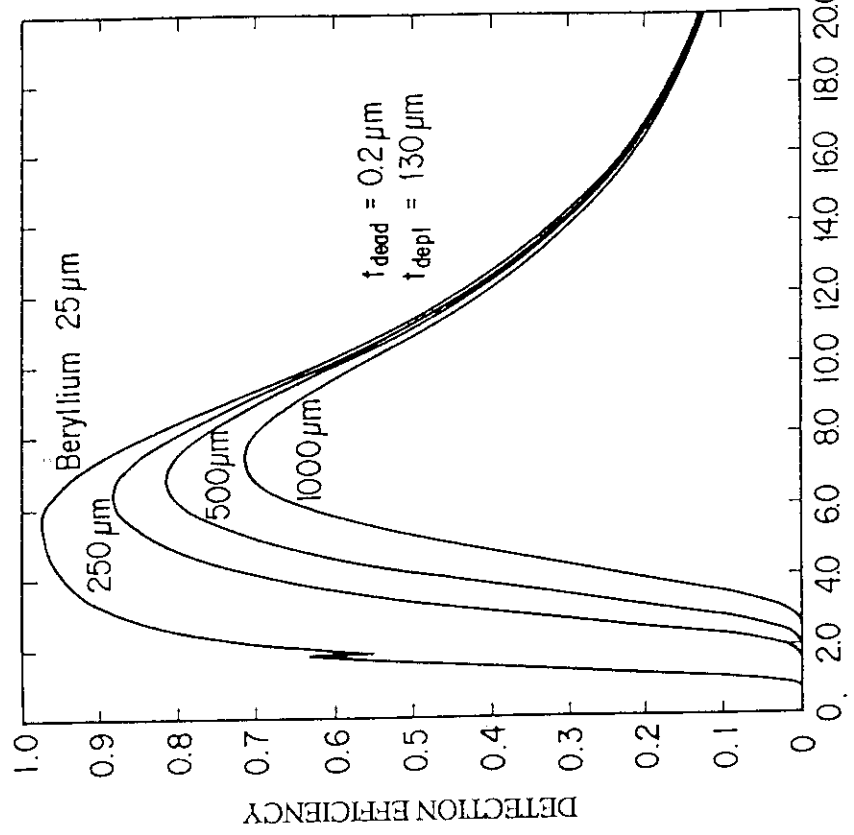

Fig.2 The calculated detection efficiency of PIN photo-diode including the filter transparency.

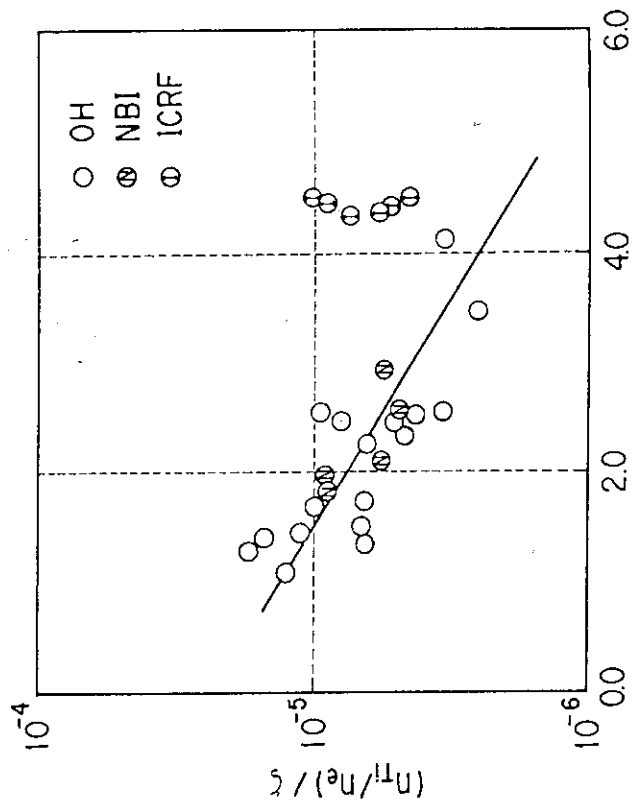

Fig.5 The density dependence of $\eta_i=(n_i/n_c)/\zeta$ in the case of titanium. The shown values were measured by the soft x-ray pulse height analysis.

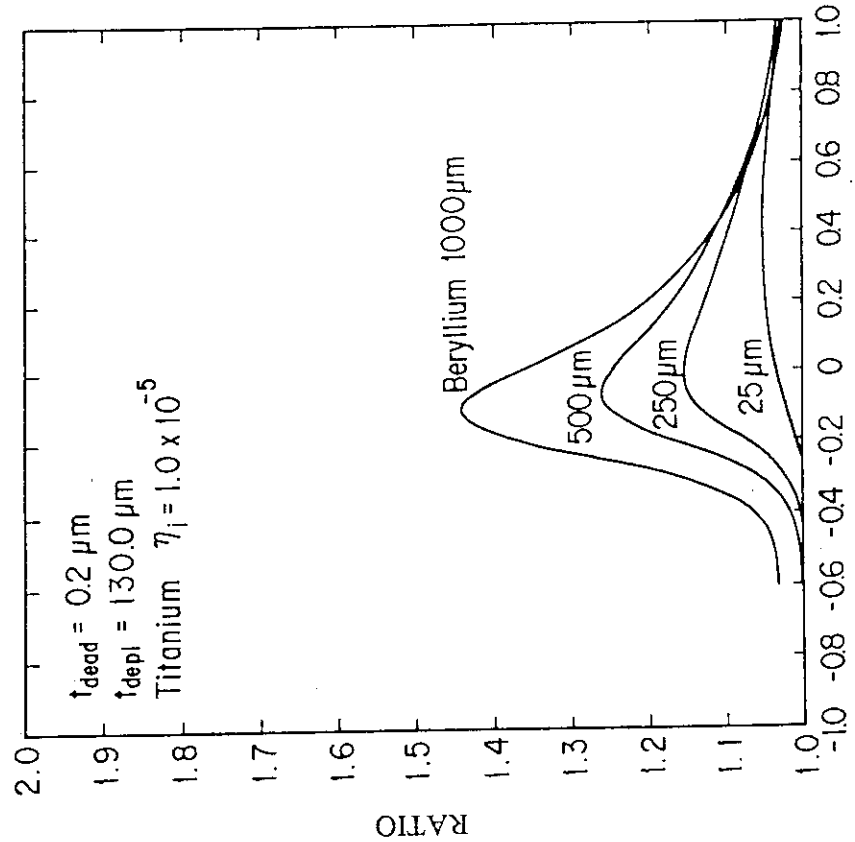

Fig.4 The dependence on the electron temperature of the ratio of the soft x-ray intensity including the line radiation to the non-including in the case of titanium Kα-line.

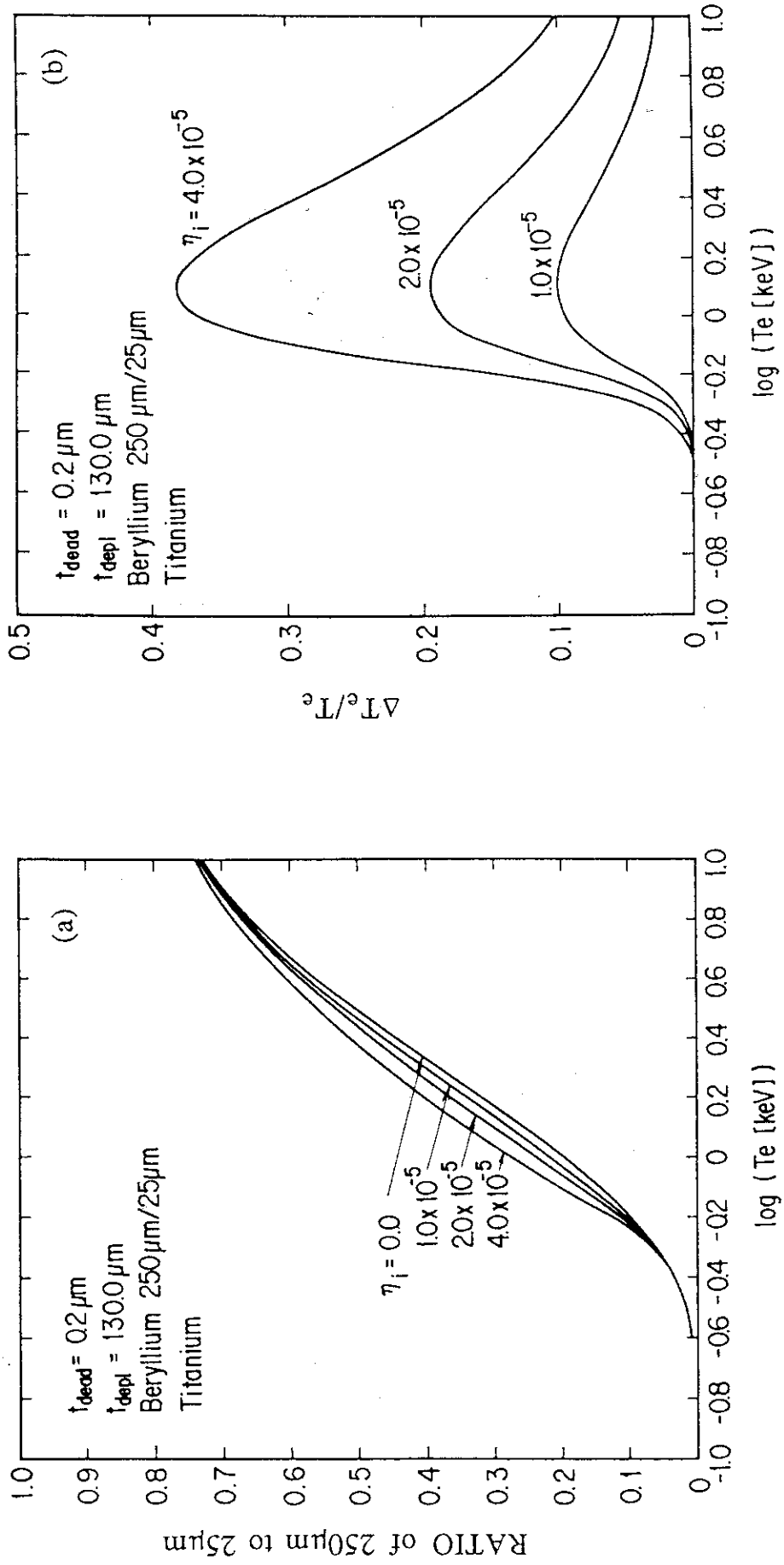

Fig.6 (a) The electron temperature dependence of the ratio of the soft x-ray intensities through the 250μm and 25μm beryllium filters. The four lines show the dependence on η_i in the case of titanium.
(b) The electron temperature dependence of the error due to the Kα-line radiation from the case of Fig.6 (a).

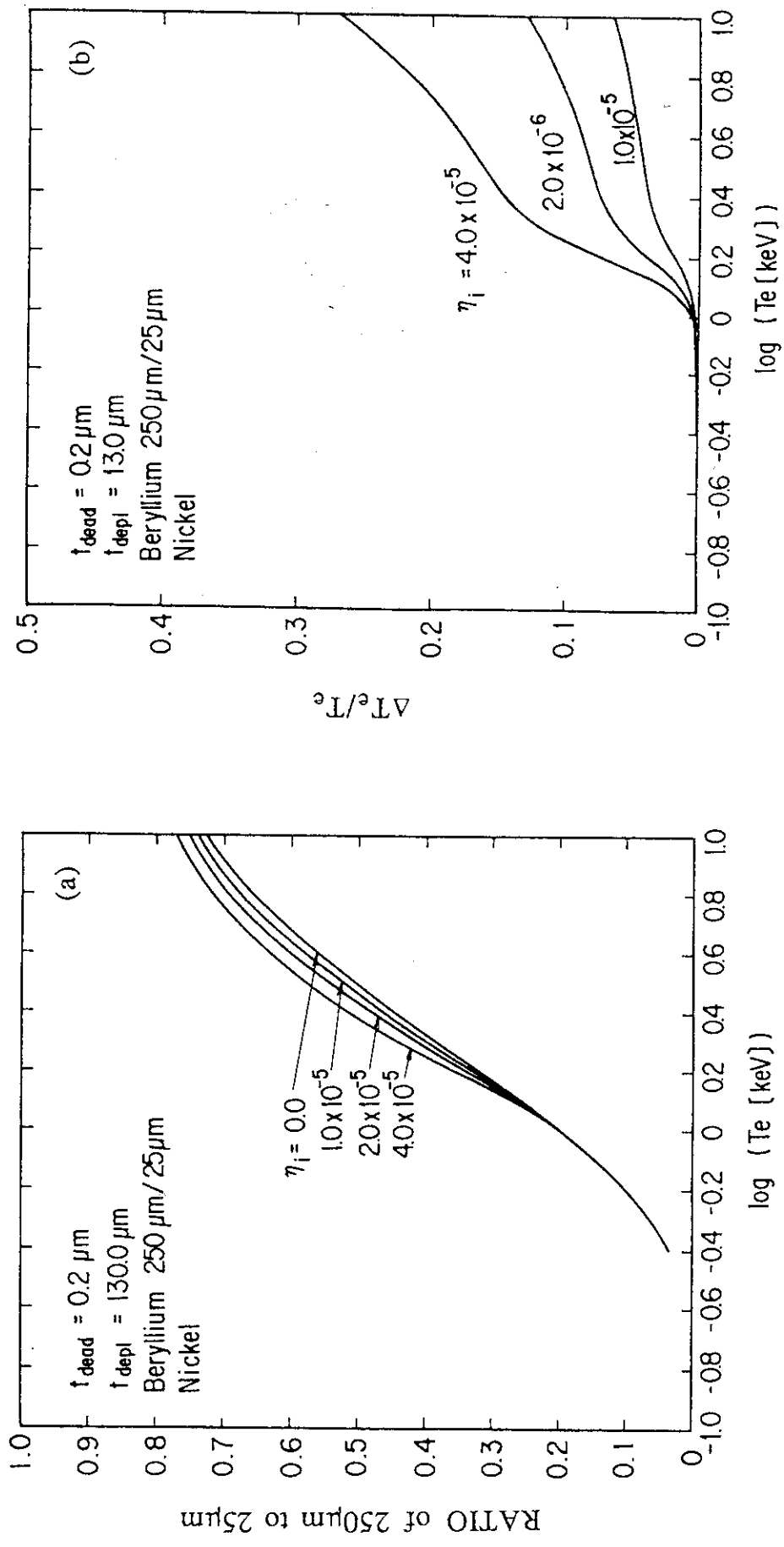

Fig.7 (a) The electron temperature dependence of the ratio of the soft x-ray intensities through the 250μm and 25μm beryllium filters. The four lines show the dependence on η_i in the case of nickel.
(b) The electron temperature dependence of the error due to the Kα-line radiation from the case of Fig.7 (a).

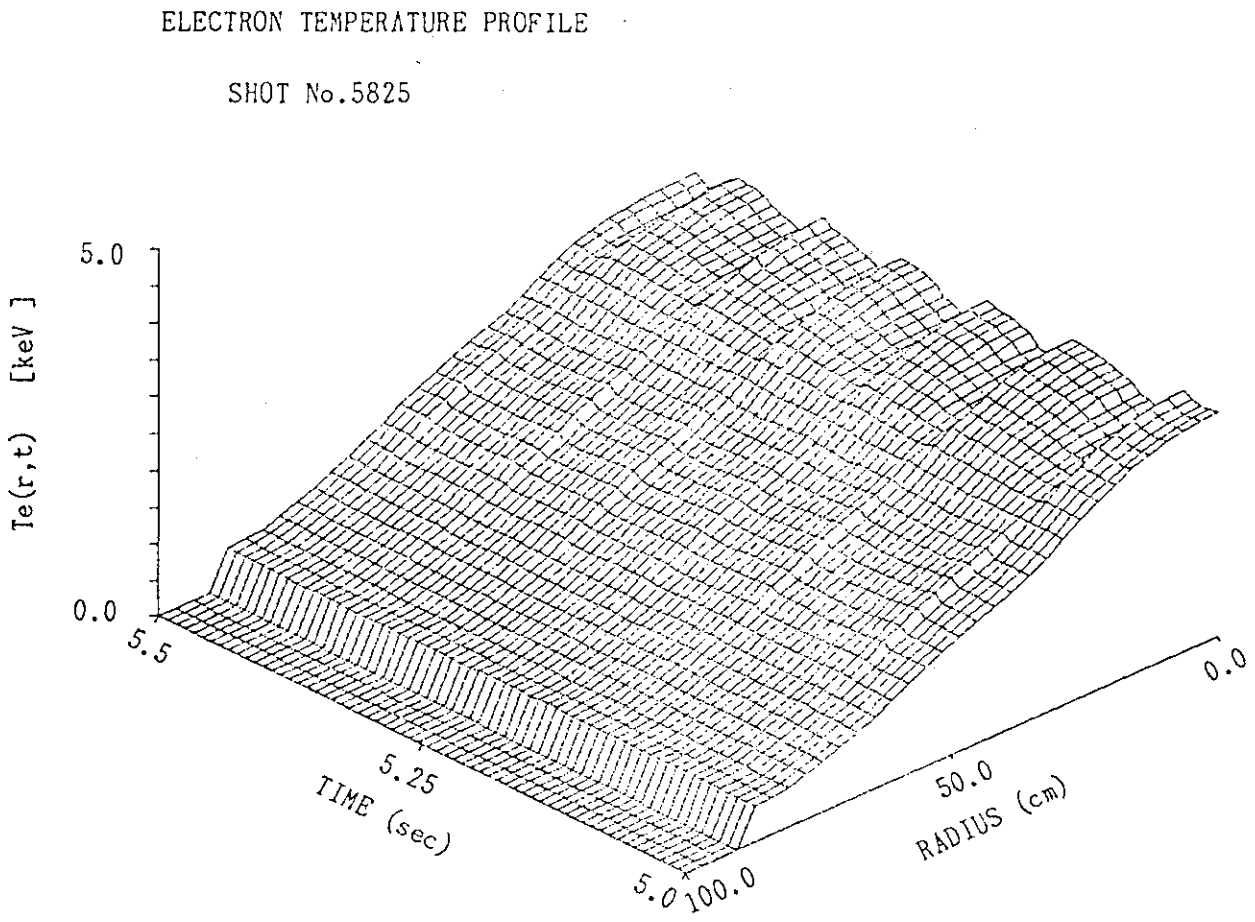

Fig.8 The time evolution of the measured electron temperature profile using the filter absorption method.

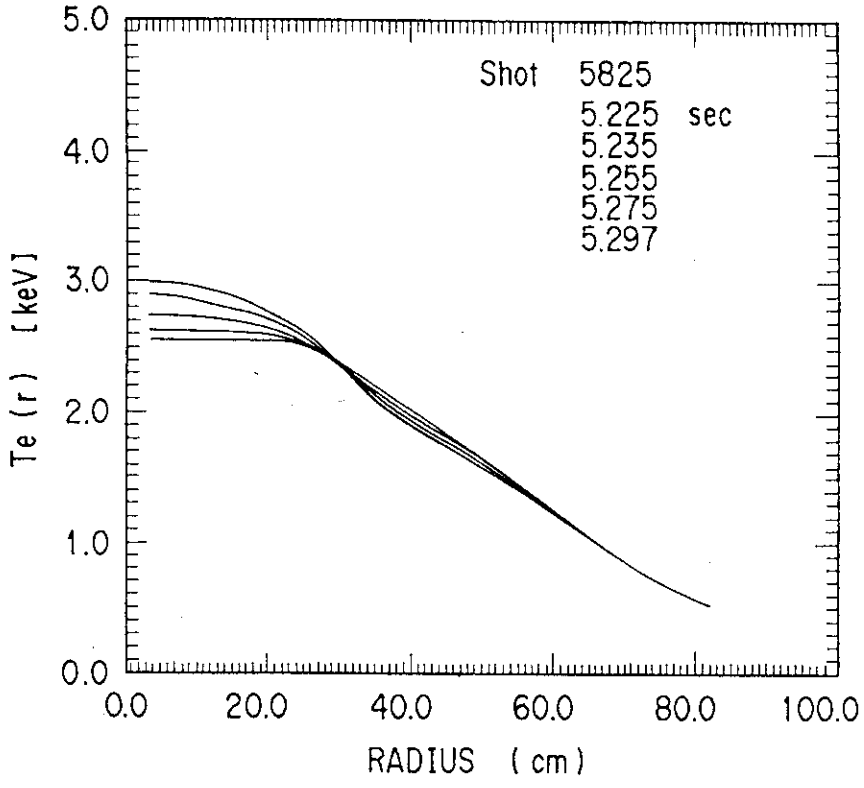

Fig.9 The electron temperature profiles of one sawtooth evolution in the case of Fig.8.

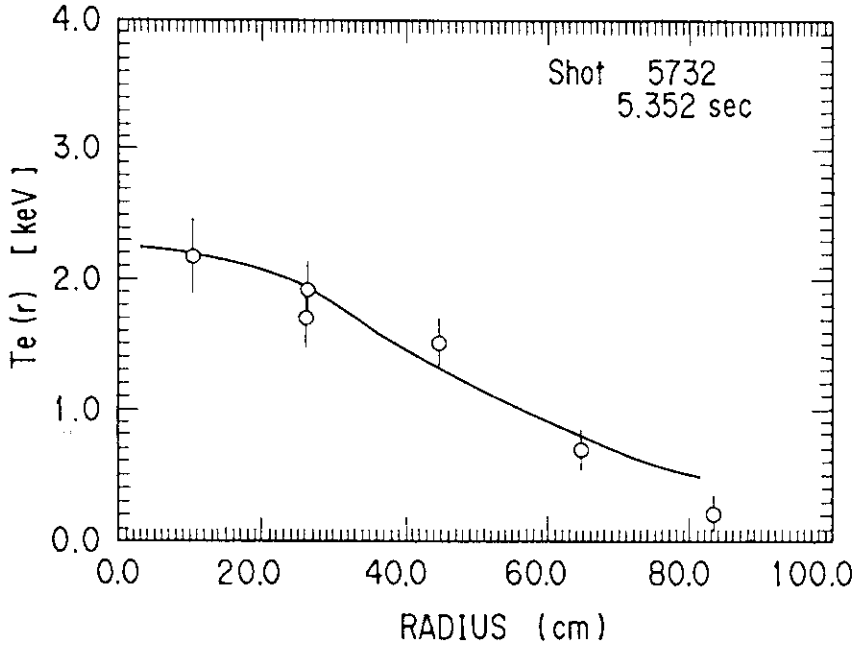

Fig.10 The comparision of the measured electron temperature profile between the filter absorption method(solid line) and the thomson scattering method(open circle).

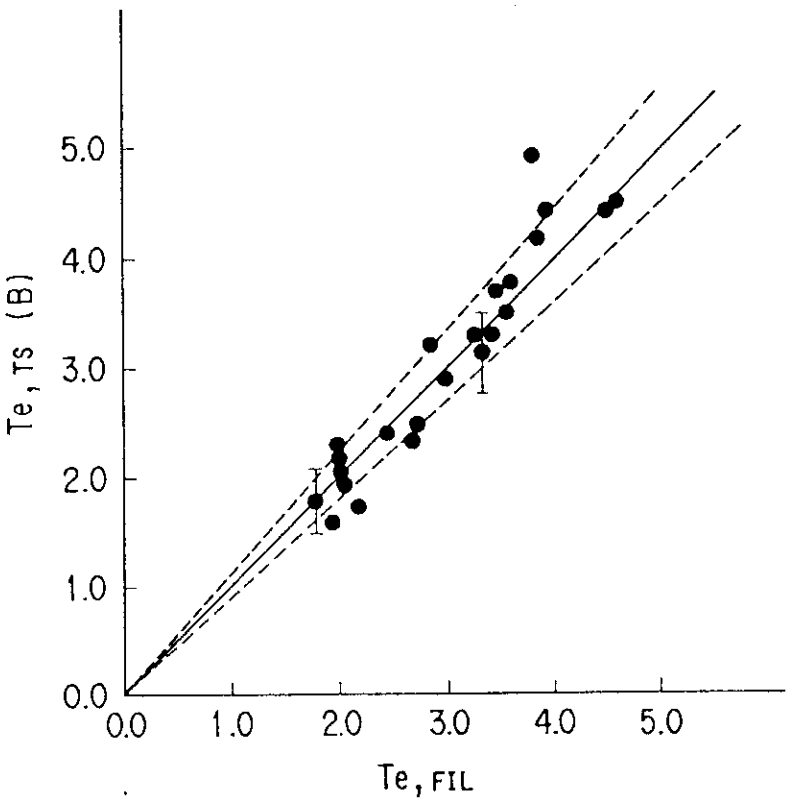

Fig.11 The comparision of the central electron temperature between the filter absorption method and the thomson scattering method.

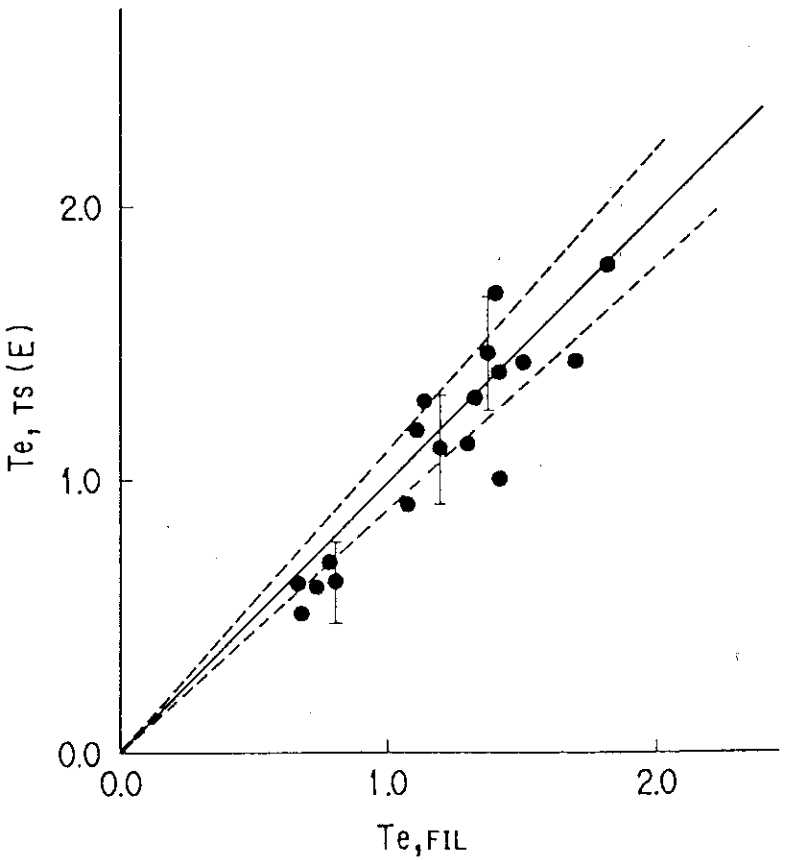

Fig.12 The comparision of the peripheral electron temperature (r=64cm) between the filter absorption method and the thomson scattering method.

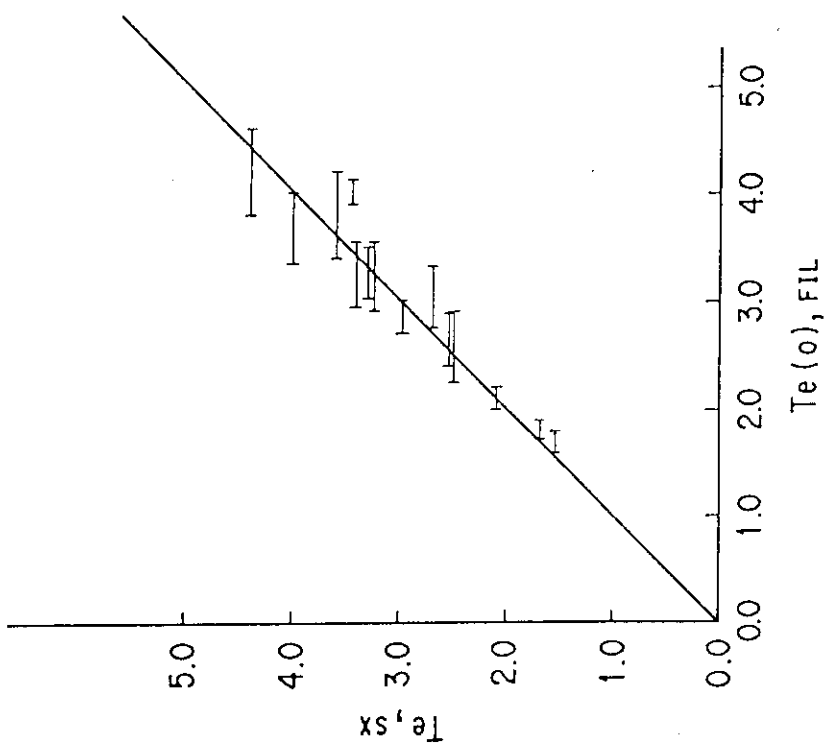

Fig.13 The comparision of the central electron temperature between the filter absorption method and the soft x-ray pulse height analysis.

APPENDIX

To obtain the solution of eqs.(6) to (9), eq(10) must be minimized by changing the valuable $x=T_e$. The relation between eq.(10) and eqs.(6)-(9) is written as follows,

$$y_j = g_j \qquad (j=1 \text{ to } J) \qquad (A.1)$$

$$f_{j0}(x) = T_e^{-1/2} F_j(T_e) \qquad (A.2)$$

$$f_{ji}(x) = G_{ji} \langle \sigma v \rangle_i'' \qquad (i=1 \text{ to } I) \qquad (A.3)$$

$$a_0 = 3.0E\text{-}15\ n_e^2\ \zeta \qquad (A.4)$$

$$a_i = a_0\ \eta_i \qquad (i=1 \text{ to } I) \qquad (A.5)$$

The values of a_i and x, which give the minimum of S(x), are the solutions. If x is given, f_{ji} can be calculated and eq.(10) is rewritten using the matrixs of Y, X and A as follows,

$$Y(k) = X(k,i)\ A(i) \qquad (i,k=0 \text{ to } I) \qquad (A.6)$$

$$Y_k = \sum_{j=1}^{J} f_{jk} y_j \qquad (A.7)$$

$$X_{ki} = \sum_{j=1}^{J} f_{jk} f_{ji} \qquad (A.8)$$

$$A_i = a_i \qquad (A.9)$$

where Y_k, X_{ki} and A_i represent the each matrix elements. Here, x is the electron temperature and a_0, $a_i (i>0)$ correspond to the continuum and line radiations.